Annual Journal of Hydraulic Engineering, JSCE, Vol.50, 2006, February

LABORATORY EXPERIMENTS ON MOISTURE CONTENT VARIATION AND LANDSLIDES CAUSED BY TRANSIENT RAINFALL

Raj Hari SHARMA[1], Hajime NAKAGAWA[2] , Yasuyuki BABA[3], Yasunori MUTO[3] and Makato ANO[4]

[1]Student Member of JSCE, Graduate Student., Graduate School of Civil Engineering and Earth Resources, Kyoto University (Yoshida-Honmach, Sakyo-ku, Kyoto 606-8501, Japan)
[2]Member of JSCE, Dr. of Eng., Professor, Disaster Prevention Research Institute, Kyoto University (Shimomisu, Yoko-oji, Fushimi-ku, Kyoto 612-8235, Japan)
[3] Member of JSCE, Dr. of Eng., Disaster Prevention Research Institute, Kyoto University (Shimomisu, Yoko-oji, Fushimi-ku, Kyoto 612-8235, Japan)
[4]Undergraduate student, Undergraduate School of Global Engineering, Kyoto University (Yoshida-Honmach, Sakyo-ku, Kyoto 606-8501, Japan)

Rain induced landslide is increasingly becoming major natural disaster. Although pore-water rise in the soil domain is taken as the cause of the landslide, it is yet not clearly known the response of pore-water pressure in different complexities of the soil domain. Multiple layers of soil with different hydraulic properties is one of the common complexities found in the field. We have tried to find out the mechanisms of moisture content variation and landslides in single and two layered slopes. The results showed that the upper layer which has higher hydraulic conductivity experiences slide first in case of two layered slope while slide of whole depth occurred in the single layered slope. A numerical model was also prepared to simulate the infiltration and landslide due to rainfall. The results as timing of landslide and moisture movement pattern from experiment and numerical simulation are quite close. The results encourage further research towards making landslide predication model.

Key Words: landslides, moisture content, numerical simulation, laboratory experiment, layered soil

1. INTRODUCTION

Landslide constitutes a major threat to both lives and properties in hilly regions of the world, which experience intense rainfall events. Rain induced landslides are causing increasing damages associated with urban development and global warming[1)]. As landslide may occur in a matter of seconds without warning during a prolonged heavy rain, it is taken as one of the most destructive natural hazards.

Rain induced landslides are caused by a reduction of confining stress that holds them, as a result of pore-water pressure rise, during or following the periods of intense rain. Due to the intense rainfall, water infiltrates to the ground reducing the matric suction. As the wetting front reaches the base where the hydraulic conductivity of the underlying layer is quite low, water table starts to rise up increasing pore water pressure which possibly lead to landslide, otherwise stable slopes.

To save the life and property from the risk of the slope failure, some sorts of prediction, which can quantitatively assign the risk to particular location and time, is essential. Numerical simulation is such a tool, which can analyze the probability of slope failure with different scenarios of rainfall and any complex soil domain.

But the current understanding of the mechanisms and conditions leading to rain induced failure is not sufficient to develop an efficient warning system[2)]. To establish the accurate warning systems, efforts have been focused on understanding the mechanism and conditions leading to these failures and on formulating procedures to predict their occurrences.

The main objective of this paper is to investigate the difference in mechanism of moisture content

Table 1 Some parameters of the sediments considered

Sediment type	S7	S8
Saturated moisture content, θ_{sat} (-)	0.528	0.467
Residual moisture content, θ_{res} (-)	0.100	0.139
α	0.943	1.149
η	1.500	1.142
Saturated hydraulic conductivity, K_{sat} (mm/hr)	315	56
Specific gravity, Gs	2.63	2.63
Mean grain size, D_{50} (mm)	0.13	0.05
Angle of repose, ϕ (degree)	34	34

variation and landslide due to rainfall, on single layer and multiple layered soil domains.

Experiments on a sloped flume were done and its result of moisture movement pattern and landslides were compared with the results of numerical simulation.

2. NUMERICAL MODEL

(1) Infiltration

Infiltration due to transient rainfall involves moisture movement through unsaturated / saturated zones. Modeling of such flow can be done using Richards equation. Richard's equation can be written as Iverson R. M.[3),4)]

$$C\frac{\partial h}{\partial t}=\frac{\partial}{\partial x}\left\{K_x(h)\left(\frac{\partial h}{\partial x}-\sin\alpha\right)\right\}+\frac{\partial}{\partial y}\left\{K_y(h)\frac{\partial h}{\partial y}\right\}+\frac{\partial}{\partial z}\left\{K_z(h)\left(\frac{\partial h}{\partial z}-\cos\alpha\right)\right\} \quad (1)$$

where, h is pressure head, C is rate of change in moisture content per unit change in pressure head ($\partial\theta/\partial h$), θ is soil volumetric water content, t is time, α is slope angle, $K_x(h)$, $K_y(h)$ and $K_z(h)$ are hydraulic conductivity in x, y and z directions (Fig.1), respectively. The hydraulic conductivities may vary owing to variations of h at the unsaturated state. At saturation they becomes saturated hydraulic conductivity K_s

In order to solve RE, the constitutive equations, which relate the pressure head to the moisture content and the relative hydraulic conductivity, are required. In this study, following constitutive relationships (Equations 2 to 4) proposed by van Genuchten are used for establishing relationship of $K-h$ and $\theta-h$, with $m=1-(1/n)$.

$$K=\begin{cases}K_sS_e^{0.5}\left[1-(1-S_e^{1/m})^m\right]^2 & \text{for } h<0\\ K_s & \text{for } h\geq 0\end{cases} \quad (2)$$

$$S_e=\begin{cases}\left(1+|\beta h|^n\right)^{-m} & \text{for } h<0\\ 1 & \text{for } h\geq 0\end{cases} \quad (3)$$

$$S_e=\frac{\theta-\theta_r}{\theta_s-\theta_r} \quad (4)$$

where, K_s is the saturated hydraulic conductivity, β and n are parameters related with matric potential of soil and are measure of capillary fringe thickness and pore size distribution of soil respectively, S_e is the effective saturation θ_s and θ_r are saturated and residual moisture content respectively.

In this study van-Genuhten parameters of soil water retention curve was determined from experiment. Some of the parameters of the sediment used in the study are given Table 1.

(2) Slope stability

An infinite slope theory was used for slope stability calculation. Safety factor (SF) is calculated for each grid with respect to resisting and driving shear stresses. Considering the two layers of soil over an impervious bed SF in each layer is calculated as a ratio of the resisting and driving shear stress developed at bottom of considered layer. The acting shear stress, τ_A and the resistance shear stress, τ_{AL}, at the interface of A/B-layer, are expressed respectively by

$$\tau_A=g\sin\alpha\cos\alpha\left[\begin{array}{l}D_A(1-\lambda_A)\sigma_A+\\ \rho\left\{\int_0^{D_A-H_A}\theta dz+H_A\lambda_A+H_s\right\}\end{array}\right] \quad (5)$$

$$\tau_{AL}=g\cos^2\alpha\left[\begin{array}{l}(D_A-H_A)(1-\lambda_A)\sigma_A\\ +\rho\int_0^{D_A-H_A}\theta dz\\ +H_A(1-\lambda_A)(\sigma_A-\rho)\\ +\rho H_s\end{array}\right]\tan\phi_A+c_A \quad (6)$$

where, A denotes the upper layer and B denotes the lower layer of soil domain.

In the same manner the acting shear stress, τ_B and the resistance shear stress, τ_{BL}, at the interface of B/C-layer, are expressed respectively by

$$\tau_B=g\sin\alpha\cos\alpha\left[\begin{array}{l}D_B(1-\lambda_B)\sigma_B+\\ \rho\left\{\int_{D_A}^{D_A+D_B-H_B}\theta dz+H_B\lambda_B+H_s\right\}\end{array}\right] \quad (7)$$

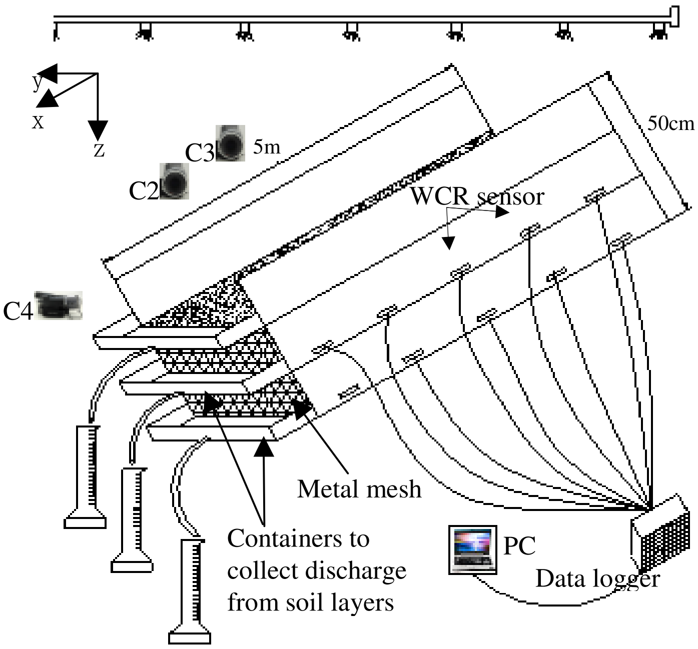

Fig. 1 Overview of experimental setup, instrumentation and data logging system. C1,C2,C3 and C4 are video cameras

$$\tau_{BL} = \left[\begin{array}{l} \tau_A \tan\phi_B / \tan\alpha + \\ + g\cos^2\alpha \left\{ \begin{array}{l} (D_B - H_B)(1-\lambda_B)\sigma_B \\ + \rho \int_{D_A}^{D_A+D_B-H_B} \theta dz \\ + H_B(1-\lambda_B)(\sigma_B - \rho) \end{array} \right\} \end{array} \right] \tan\phi_B + c_B \quad (8)$$

where, D and H are thickness and seepage flow depth on soil layers and H_s is surface flow depth. Similarly $\lambda, \sigma, \rho, \phi$ and c are porosity of a soil layer, density of a sediment particle, density of water, angle of repose and cohesion respectively. g is acceleration due to gravity. Subscripts A or B denotes a value in A layer or B layer. When, $H_A \geq D_A$, it is set that $H_A = D_A$ and when $H_B \geq D$, the following equation is used instead of Eq.(8).

$$\begin{aligned} \tau_{BL} &= (\tau_{AL} - c_A)\tan\phi_B / \tan\phi_A \\ &+ g\cos^2\alpha D_B(1-\lambda_B)(\sigma_B - \rho)\tan\phi_B + c_B \end{aligned} \quad (9)$$

The safety factor SF_A and SF_B for A and B layer respectively are function of time dependent parameters H_A, H_B and H_s. SF for each layer is calculated using following equation;

$$\begin{aligned} SF_A &= \tau_{AL} / \tau_A \\ SF_B &= \tau_{BL} / \tau_B \end{aligned} \quad (10)$$

The area having SF less then 1 is assumed to have landslide.[4)]

3. LAB EXPERIMENT

(1) Set-up of the experimental flume

A series of slope failure experiments was conducted to examine the initiation of rain induced slope failure and the process of moisture movement before the actual failure occurs. A flume of 5m long, 0.3m wide, and inclined at an angle of 30^{o} was used Fig. 1 shows the schematic diagram of the flume, instrumentation and data acquisition systems. The sidewall of the flume was made from transparent aquarium glass so that the soil slide can be captured by a video camera from the side. The soil depth was kept 10 cm to 20 cm in different cases. Rain at the rate of 100-200 mm/h was applied to the slope segment during the experiment by a large indoor type rainfall simulator, which has different types of sprinkling nozzles. The relationship of the pump rate and the rainfall rate at actual ground was first established by using 5 rain gauges placed just at the level of the sloped flume in regular intervals.

Campbell-water content reflectometer (WCR) measured the temporal variation in moisture content during the infiltration of rainwater. 10 to 12 number of WCR were inserted to the sand horizontally from a sidewall of the flume. The data acquisition interval for WCRs was 1 min.

To measure the soil movement at the time of landslide, red colored sediment was placed in six different vertical strips (1cm*1cm) at the face of the flume wall opposite to that contains WCR. Three digital video cameras (C1, C2, C3) were placed on the side of the flume wall opposite to that contains WCRs i.e. the same side as with colored sands. Those three pairs of video cameras were adjusted to film three parts of the experimental area from bottom to top from side. Another camera C4 was placed above the sloped flume. A stopwatch was used to record the start of experiment.

The downstream boundary was maintained with free flow condition. Iron meshes each of 5cm height was kept to full width of flume to retain soil inside the flume. The opening of the mesh was 0.1mm. The downstream of the flume was connected with water containers to collect the flow from the different layers of the soil domain (Fig. 1). Those metal containers were connected to the measuring container by pipe. Upstream end was closed with wooden block.

The flume was initially covered with plastic and was lifted up after about 10min of the start of the rainfall simulator to achieve uniform rainfall throughout the experiment.

(2) Calibration of WCR

WCR is designed to measure volumetric water content of soils or other porous media. The WCR method for measuring soil water content is an

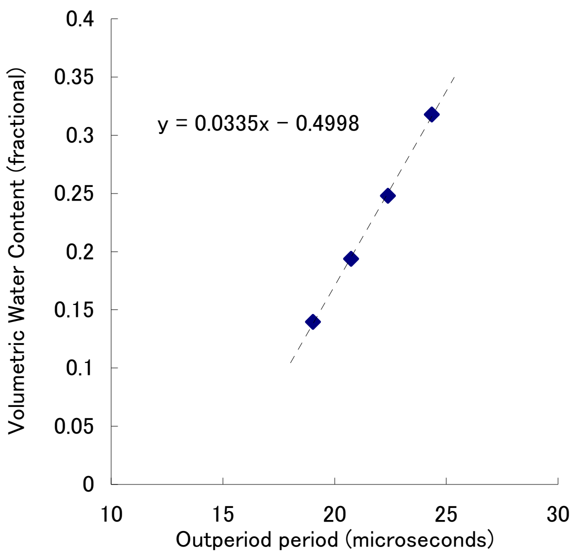

Fig. 2 Typical quadratic calibration curve for WCR-1 and S8

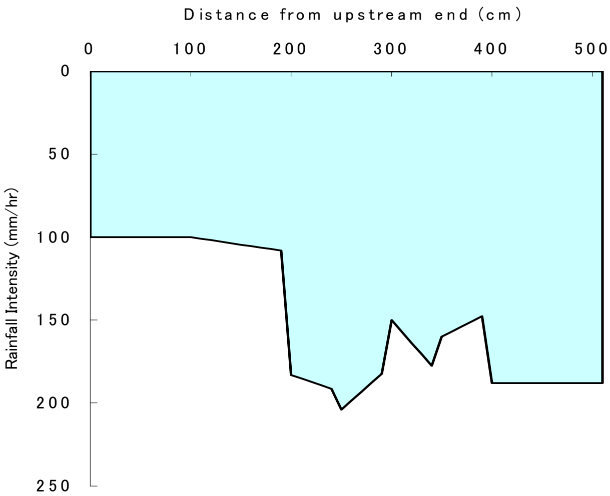

Fig. 3 Distribution of applied rainfall

indirect measurement that is sensitive to the dielectric permittivity of the material surrounding the probe rods. The probe rods can be inserted at any orientation to the surface. A probe rod installed horizontal to the surface can detect the passing of wetting fronts or other vertical water fluxes. The rod should be installed parallel as in original position.[5]

The fundamental principle is that an electromagnetic pulse will propagate along the probe rods at velocity that is dependent on the dielectric permittivity of the material surrounding the line. As water content increases, the propagation velocity decreases because polarization of water molecules takes time.[5]

Since output period is different for different soil and different degree of compaction, a unique calibration should be done prior to the experiment. Campbell Inc. has suggested using quadratic or linear equation to describe probe output response to changing water content. Two data points for linear

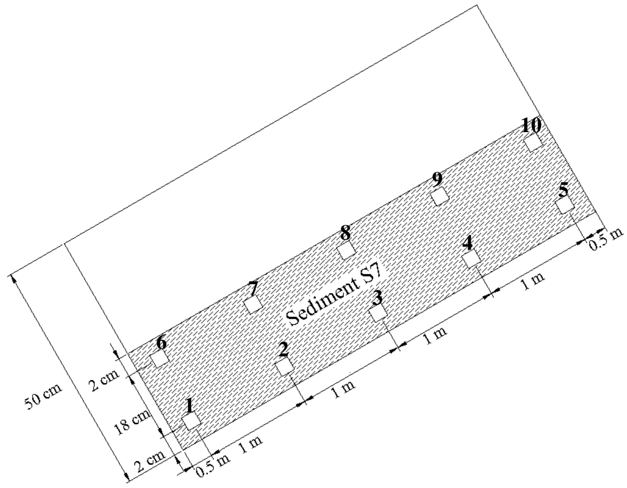

Fig. 4 Arrangement of WCRs (1-10) in experiment I (only one layer of S7 was used)

calibration and three for quadratic calibration are essential. With three evenly spaced water contents covering the expected range, the middle water content data point will indicate whether a linear or quadratic or linear equation is needed.[5] Fig. 2 shows a typical calibration curve of WCR-1 for S8 and its calibration equation. In this case linear calibration was chosen because a straight line can connect all the four points.

4. RESULTS AND DISCUSSION

Two experiments were done with different conditions. One was with single layer silica sand S7 and the other was two layers with silica S7 overlaying silica S8, both at an angle of 30°. Table 1 shows some properties of S7 and S8.

Artificial rainfall was sprinkled over the entire exposed slope surface. Monitoring the rainwater prior to the experiment-using bucket just above the experimental flume was done in every 0.5m interval to rechecked actual rainfall intensity. The pattern of rainfall in the entire region is quite varying from 100mm/hr to 209mm/hr. Fig. 3 shows the rainfall pattern above the flume for both experiments. Numerical simulation of the process of infiltration and landslide were also done for both cases.

(1) Case I: single layer of sediment

The slope was set with the relatively dry sediment S7 in one layer. The deposit thickness was 20cm. Artificial rain (Fig.3) was applied to the flume. 10 Sensors were placed in different position of the flume to capture the entire moisture within the flume. Fig. 4 shows the arrangements of WCRs. The top five WCR were placed (6,7,8,9 and 10) at 2cm down from the sand surface and bottom five (1,2,3,4 and 5) were placed at 2cm up from bottom face of flume as shown in fig.4.

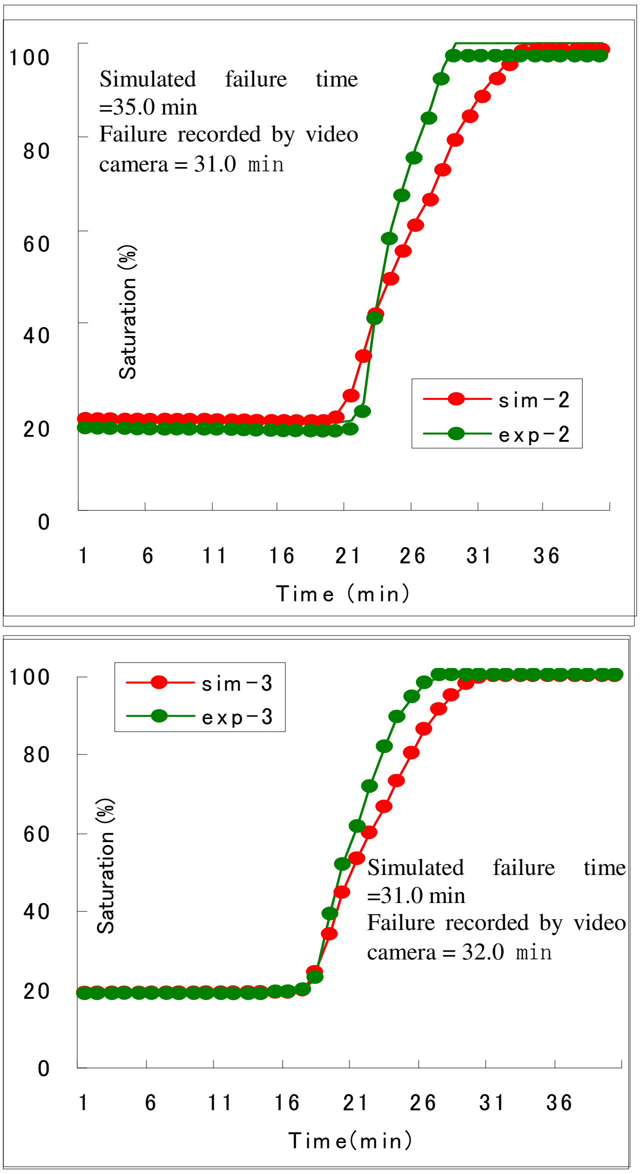

Fig.5 Numerical Simulation and experimental result of moisture Saturation (%) on single layered soil

The time to reach the moisture content in every sensor even in the same distance from top surface were different due to the slope of the flume and uneven distribution of the rainfall.

Figure 5 shows the experimental and numerical simulation result of the moisture movement at WCR-2 and WCR-3, which are close to base and experience failure first. After the wetting front reaches the base the groundwater table starts to rise up and the landslide occurs. The result shows that the numerical and simulated values are quite close.

From the video camera start of tilting of the red color strips had been seen at 31 min near WCR-2 and at 32 min near WCR-3. The simulated results shows that they are at 35 min and 31 min at WCR-2 and WCR-3. Complete movement of the soil mass occurred only after some minutes of the start of the failure process.

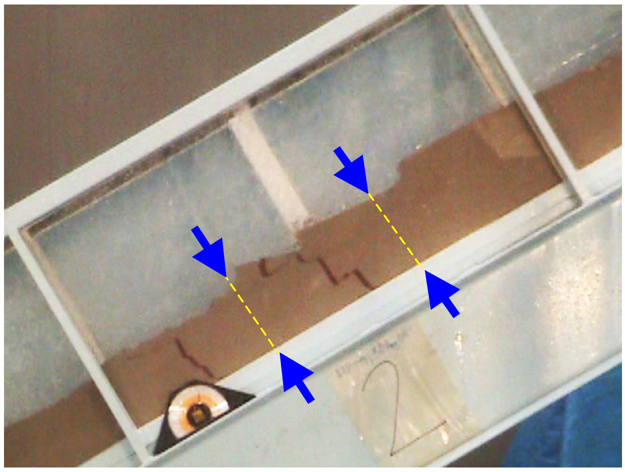

Fig. 6 Slide of whole 20cm depth in first experiment; yellow lines (between blue arrows) show original positions of red strips (initially 1.33m and 1.66m from downstream end)

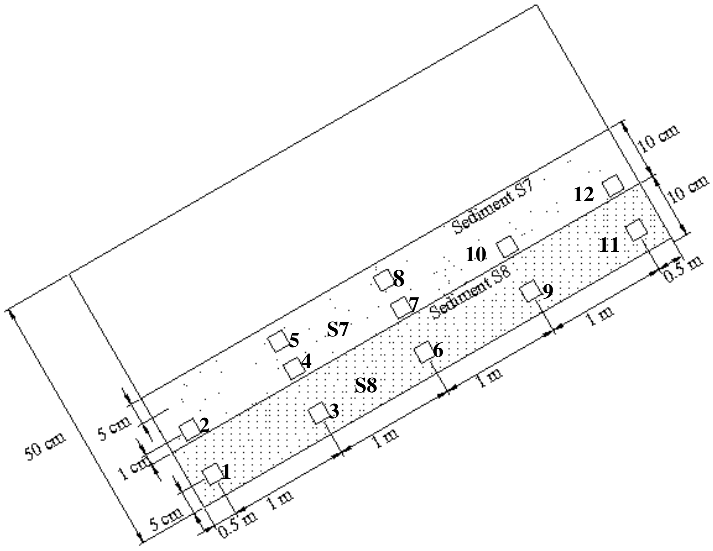

Fig. 7 Arrangement of WCRs (1-12) in experiment II (upper layer S7 and lower layer S8)

Fig. 6 shows the initial and final position red sand strips indicating landslide. It shows complete collapse of the slope in 20cm, which means that water table starts to rise up from the impermeable base at the bottom of the slope. This causes slide of whole depth.

(2) Case II: Two layers of sediment

The slope in this two layered sediment model also had the slope angle of 30°. Lower layer 10cm depth was S8 while upper 10 cm was S7 sand. All WCRs were placed in different position (Fig. 7) so that the moisture movement pattern in upper layer and lower layer both could be captured. The rainfall was supplied with the intensity as shown in Fig.3. Throughout the experiment moisture content of the soil slope increased slowly with time towards a saturated value in response to increase in wetting front of rainwater and increasing groundwater level.

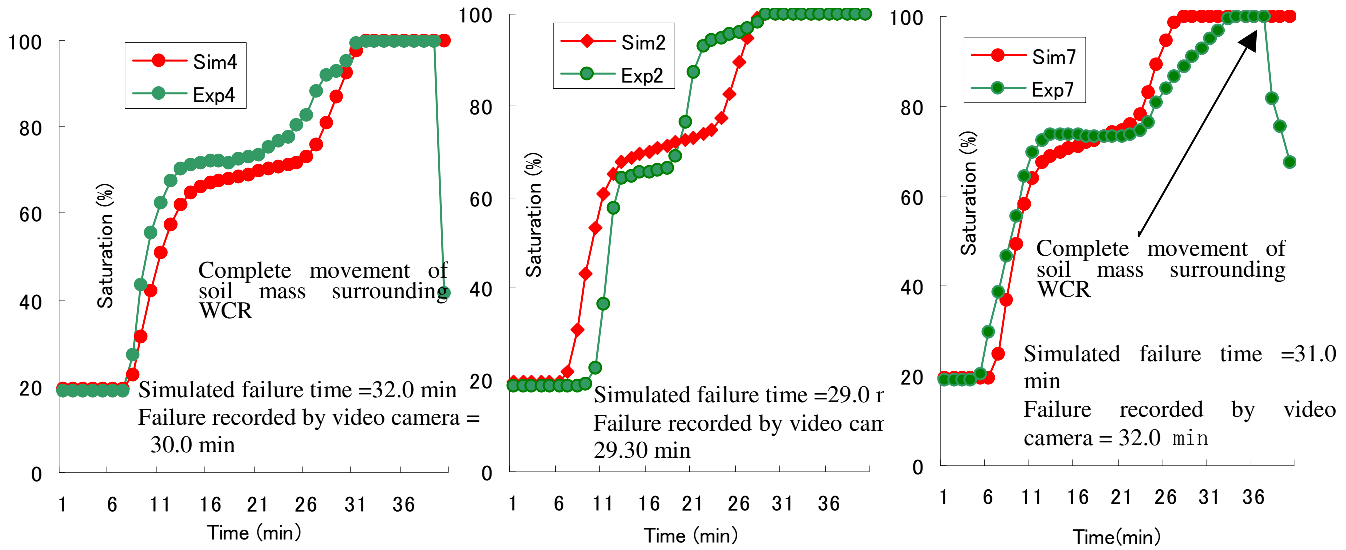

Fig.8 Experimental and simulated results of the water content profile and landslide time (WCR-4, 2and 7)

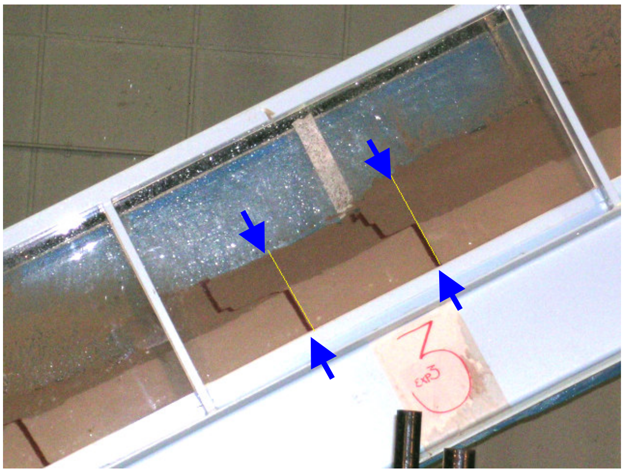

Fig.9 Upper layer fails in second experiment; yellow lines (between blue arrows) show original positions of red strips (initially 2.33m and 2.66m from downstream end)

Fig. 8 shows the numerical and experimental simulation of the temporal water content profile and the timing of landslide. In this case the failure on the upper layer consisting of S7 occurs first. The numerical and simulated moisture content profile are very close to each other for all WCRs. Simulated and experimental failure time are also quite close to each other. Complete slide can also be dictated from fig.8 at the WCR-4 and WCR-7, which were due to the exposure of WCR probes to air after movement of whole soil mass surrounding them. But the actual failure i.e. start of tilt occurs some minutes before the complete collapse which was captured by video camera. Overlaying the initial state of the sand strips on final stage at different time steps helped to find the start of the tilt of red sand strips.

From Fig.9 it is obvious that the failure depth is just 10 cm in this case. Only top 10 cm of S7 sediment, which has high hydraulic conductivity, slides and bottom 10cm of S8 sediment remains in its original position.

5. CONCLUSION

Two distinct failure mechanisms were found in the experiments. In the case of the single layered slope, water table rises up from the bottom impervious layer at 20cm depth and whole 20cm depth of sand slides. However, in the case of the two-layered slope only the top layer of sand with 10cm depth slides. Due to the smaller hydraulic conductivity of the under laying sand, water table rises up from the bottom of upper layer which causes failure of the upper layer only. It helps to conclude that depth of failure depends highly on the layering characteristics of the soil domain in the field. The results of numerical simulation and laboratory experiments of temporal changes in moisture movement and landslide are quite comparable. It shows the potential of the numerical model to be extended for the use in real field.

ACKNOWLEDGMENT: We wish to thank Dr. K. Kosugi and Dr. D. Tsutsumi for their help in measurement of soil hydraulic properties.

REFERENCES

1) Moriwaki, H., Inokuchi, T., Hatanji, T., Sassa, K., Ochiai, H., and Wang, G.: Failure processes in a Full Scale Landslide Experiment using Rainfall Simulator, *Landslides*, Vol.1, pp.277-288, 2004.
2) Ornse, R. P., Shimoma, S., Maeda, K., and Towhata, I.: Instrumented Model Slope failure due to water Seepage, *J. Natural Disaster Science*, Vol.26 (1), pp.15-26, 2004.
3) Iverson R. M.: Landslide Triggering by Rain Infiltration, *Water Res. Research*, Vol.36(7), pp.1897-1910, 2000.
4) Sharma, R. H. and Nakagawa, H.: Predicting timing and location of rainfall triggering shallow landslides, *Annual J. of Hydraulic Engineering*, JSCE, Vol. 49, pp.43-48, 2005.
5) Campbell Scientific Inc.: In CS616 and CS625 *Water Content Reflectometers,* Instruction Manual, 2004.

(Received September 30,2005)